Effect of ultra-wide-band electromagnetic pulses on blood-brain barrier permeability in rats

PENG GAO[1*], QIN CHEN[1,2*], JUNFENG HU[1], YANYUN LIN[1], JIAJIN LIN[1], QIYAN GUO[1], HAO YUE[1], YAN ZHOU[1], LIHUA ZENG[1], JING LI[1], GUIRONG DING[1] and GUOZHEN GUO[1]

[1]Department of Radiation Medicine and Protection, Faculty of Preventive Medicine, Airforce Medical University, Xi'an, Shaanxi 710032; [2]Department of Infection Prevention and Control, General Hospital of Western Military Region, Chengdu, Sichuan 610083, P.R. China

Received February 27, 2020; Accepted June 25, 2020

DOI: 10.3892/mmr.2020.11382

Abstract. The restrictive nature of the blood brain barrier (BBB) brings a particular challenge to the treatment of central nervous system (CNS) disorders. The effect of ultra-wide band electromagnetic pulses (UWB-EMPs) on BBB permeability was examined in the present study in order to develop a safe and effective technology that opens the BBB to improve treatment options for CNS diseases. Rats were exposed to a single UWB-EMP at various field strengths (50, 200 or 400 kV/m) and the BBB was examined using albumin immunohistochemistry and Evans blue staining at different time periods (0.5, 3, 6 and 24 h) after exposure. The expression and distribution of zonula occludens 1 (ZO-1) were evaluated using western blotting to identify a potential mechanism underlying BBB permeability. The results showed that the BBB permeability of rats exposed to UWB-EMP increased immediately following UWM-EMP treatment and peaked between 3 and 6 h after UWB-EMP exposure, returning to pre-exposure levels 24 h later. The data suggested that UWB-EMP at 200 and 400 kV/m could induce BBB opening, while 50 kV/m UWB-EMP could not. The levels of ZO-1 in the cerebral cortex were significantly decreased at 3 and 6 h after exposure; however, no change was observed in the distribution of ZO-1. The present study indicated that UWB-EMP-induced BBB opening was field strength-dependent and reversible. Decreased expression of ZO-1 may be involved in the effect of UWB-EMP on BBB permeability.

Correspondence to: Professor Guirong Ding or Professor Guozhen Guo, Department of Radiation Medicine and Protection, Faculty of Preventive Medicine, Airforce Medical University, 169 Changle West Road, Xi'an, Shaanxi 710032, P.R. China
E-mail: dingzhao@fmmu.edu.cn
E-mail: guozhen@fmmu.edu.cn

*Contributed equally

Key words: blood brain barrier, electromagnetic radiation, electric field strength, zonula occludens 1

Introduction

An increasingly aging population and deterioration in the quality of the environment are contributing to the increased incidence of central nervous system (CNS) diseases such as stroke, traumatic brain injury, brain tumors and neurodegenerative disorders (1). According to previous statistics, in 2015 the number of mortalities and disability-adjusted life-years from neurological disorders were 9.40 and 250.7 million individuals, respectively, which suggests that CNS diseases are amongst the leading causes of disability and mortality worldwide (2). It is reported that the median survival of patients with glioblastoma is only 4-15 months, and the 5-year survival rate is <5% (3). One of the reasons for the poor therapeutic effect of drugs used in the treatment of CNS diseases is that they cannot effectively be delivered to the lesions in the brain due to the blood-brain barrier (BBB) (4). The BBB consists of non-fenestrated brain microvascular endothelial cells (BMECs), which form the lining of brain capillaries, and adjacent cells including astrocytes and pericytes (5). BMECs are highly specialized structures due to their extensive tight junctions (TJs) between them (6). They play an important role in BBB function by restricting and precisely regulating the exchange of molecules between the peripheral circulatory system and CNS (7). Consequently, as a result of the presence of the BBB, numerous drugs with a molecular weight of >400 Da cannot reach the lesions in the brain (8), severely reducing the therapeutic effect of drugs used in the treatment of CNS diseases. Therefore, safe regulation of the permeability of the BBB has become a key issue in the treatment of CNS diseases.

During previous decades, various methods have been evaluated to overcome the problems associated with BBB permeability, such as local delivery strategies to bypass the BBB and physical mechanisms to breach the BBB (8). The former, which is extremely invasive, primarily refers to convection-enhanced delivery (CED) that uses positive pressure to inject anti-cancer agents directly into brain tumors and thus bypass the BBB (9). The latter includes focused ultrasound, photodynamic therapy and electromagnetic microwave pulsed (EMP) radiation (10). All these processes have been reported to open the BBB reversibly in a less invasive

manner than CED (11-13). However, focused ultrasound and photodynamic therapy must be used with microbubbles and photosensitizers, respectively, which makes these two methods more complicated and higher-risk (14,15).

Our previous studies demonstrated that *in vivo* (non-invasive) exposure of rats to EMP with a field strength of 200 kV/m and a pulse width of 14 nsec caused a temporary and reversible increase in BBB permeability; the permeability peaked at 3 h after EMP exposure (13). Moreover, the transendothelial electrical resistance of an *in vitro* BBB model, established by co-culturing primary rat BMECs and astrocytes, is lower after EMP exposure, which indicates increasing BBB permeability (16,17). Li *et al* (18) also reported that exposure of rats to EMP facilitated lomustine to penetrate the BBB and be delivered the site of a brain tumor. Nevertheless, for clinical application of EMP, it is important to evaluate the relationship between the biological effect of EMP and parameters such as electric field strength and exposure duration. Compared with traditional EMP, ultra-wide band EMP (UWB-EMP) exhibits a shorter rise time (within the psec range), higher instantaneous peak power and wider spectrum (19). Thus far, there have been very few studies focusing on the effects of UWB-EMP on BBB permeability. In the present study, a range of EMP field strengths and post-exposure durations were used to examine the potential of UWB-EMP to alter BBB permeability in rats with the aim of facilitating the development of techniques to be applied in clinical settings.

Materials and methods

Animals. A total of 138 male Sprague-Dawley (SD) rats, weighing 220±20 g (age, 7 weeks), were obtained from the Laboratory Animal Center of Air Force Medical University. Rats were acclimatized for 1 week, and housed in groups of 6 in polycarbonate cages under a 12:12-h light-dark cycle, 60% humidity and a temperature of 23±2˚C with *ad libitum* access to food and tap water. They were fasted for 12 h prior to use in the experiments, which were conducted in accordance with the National Institutes of Health Guide for the Care and Use of Laboratory Animals (20) and approved by the Animal Experimentation Ethics Committee of Airforce Medical University (approval no. IACUC-20180503).

UWB-EMP exposure and experiment protocols. The UWB-EMP exposures were conducted in a microwave chamber which housed the UWB-EMP generator (Northwest Institute of Nuclear Technology) and a platform to place animals. During exposure, rats were kept individually in a special transparent polymethyl methacrylate box (6x6x20 cm) and placed on the platform. UWB-EMP pulses were generated by a spark gap pulse generator and transmitted as previously described (21). The pulse repetition rate was 10 Hz and the pulse duration was 0.9 nsec. Appropriate electric field strength was achieved by modifying the distance between the UWB-EMP generator and the platform.

The first experiment was conducted to investigate BBB permeability at different time periods following a single UWB-EMP exposure at 400 kV/m (total 20,000 pulses). A total of 90 SD rats were randomly divided into 5 groups (n=18/group, evenly split for Evans blue (EB) staining, immunohistochemistry and western blotting): Group 1, sham exposure (without UWB-EMP transmission in the same microwave chamber); and groups 2-5, examination of BBB at 0.5, 3, 6 and 24 h, respectively, after a single UWB-EMP exposure at a field strength of 400 kV/m for 20,000 pulses.

A second experiment was conducted to investigate the effect of different field strengths of UWB-EMP on BBB. A total of 48 SD rats were randomly divided into 4 groups (n=12/group, evenly split for EB staining and albumin immunohistochemistry): Group 1, sham exposure (without UWB-EMP transmission in the same microwave chamber); and groups 2-4, UWB-EMP exposure at a field strength of 50, 200 and 400 kV/m for a total of 20,000 pulses, respectively. Thus, the average specific absorption rates of groups 2-4 were $1.10x10^{-4}$, $1.75x10^{-3}$ and $7.01x10^{-3}$ W/kg, respectively. The BBB permeability was examined at 3 h after UWB-EMP exposure.

All animals were anesthetized by intraperitoneal administration of 1% sodium pentobarbital (45 mg/kg). In the first experiment, animals were sacrificed at different time periods after UWB-EMP exposure according to the grouping. In the second experiment, animals were sacrificed at 3 h after exposure, prior to subsequent procedures, including cardiac puncture and perfusion.

EB staining. EB staining is frequently used as a marker to evaluate BBB opening due to its ability to bind to plasma albumin (22). At 30 min prior to sacrifice, each animal was injected intravenously (4 ml/kg) with 4% EB (MP Biomedicals, LLC). After perfusion with 0.9% normal saline and subsequently 4% paraformaldehyde, brains were removed and frozen at -80˚C, and then embedded in Tissue-Tek® O.C.T.™ cryostat-embedding compound (Sakura Finetek USA, Inc.). Brains were sectioned at a thickness of 30 μm. Randomly selecting six visual fields, EB extravasation was visualized using a fluorescence microscope (Leica Microsystems GmbH; total magnification, x400) with green light excitation. Quantification was performed using a scoring system by three experienced, blinded, independent lab technicians as previously described (13). Briefly, four frozen sections containing the frontal cortex from each rat were selected and a total of 24 sections were examined in each group. The comprehensive score (CS) of EB leakage was determined based on: i) Quantity of EB fluorescence spots; ii) intensity of fluorescence; and iii) range of fluorescence spots. Fluorescence range and intensity were divided into four levels from weak to strong as follows: Negative, 0; small range/weak intensity; 1; moderate range/intensity, 2; large range/strong intensity, 3. The CS of EB leakage for each section was obtained by adding the quantity of EB spots, the value for EB intensity and the value for EB range. The average score of 4 sections was the final CS of EB leakage for each rat.

ELISA. Blood was collected from each rat via cardiac puncture prior to perfusion. Whole blood samples were stored at 4˚C overnight to separate serum via natural precipitation. A rat S100β ELISA kit (sensitivity of 37.5 pg/ml; cat. no. E-EL-R0868; Wuhan Elabscience Biotechnology Co., Ltd.) was used to measure serum S100β levels according to the manufacturer's instructions. The absorbance of the

final yellow product was detected spectrophotometrically at 450 nm wavelength (Bio-Rad Laboratories, Inc.) and the optical density values were converted into concentrations via a standard curve.

Immunohistochemistry. After anesthesia and perfusion, the brains were dissected and fixed in 4% paraformaldehyde at room temperature overnight. Paraffin-embedded sections with a thickness of 5 μm were prepared, dewaxed and hydrated. Hydrogen peroxide-methanol solution (3%) was used to eliminate the endogenous peroxidase activity at room temperature for 15 min, and 0.01 M citrate buffer was used for antigen retrieval in the microwave. Sections were washed three times with PBS and blocked with 5% normal donkey serum (cat. no. SL050; Beijing Solarbio Science & Technology Co., Ltd.) in PBS at room temperature for 30 min. Then, the slides were incubated with sheep anti-albumin antibody (1:500; cat. no. A110-134A; Bethyl Laboratories, Inc.) and rabbit anti-zonula occludens 1 (ZO-1) antibody (1:100; cat. no. 61-7300; Zymed; Thermo Fisher Scientific, Inc.) at 4˚C overnight. After washing with PBS, horseradish peroxidase (HRP)-conjugated donkey anti-sheep antibody (1:500; cat. no. ab6900; Abcam) or FITC-conjugated goat anti-rabbit antibody (1:100; cat. no. A22120; Abbkine Scientific Co., Ltd.) was added to the slides and incubated for 2 h at room temperature. For albumin immunohistochemistry, the color was developed using 2,2'-diaminobenzidine (Boster Biological Technology) at room temperature for ~5 min. Following hematoxylin counterstaining (room temperature; 1 min), slides were sealed with neutral gum. A total of 24 sections in each group were observed and photographed using a light microscope (Nikon Corporation; total magnification, x400). Semi-quantitative evaluation of albumin immunohistochemistry was conducted in a similar manner to quantification of EB fluorescence.

Western blot analysis of ZO-1 and heat-shock protein 70 (HSP70). Brains were immediately dissected after euthanasia, and the cortex was separated on ice and stored at -80˚C. The total protein in the cortex was obtained with a whole protein extraction kit (cat. no. KGP250; Nanjing KeyGen Biotech Co., Ltd.) and then quantified using a bicinchoninic acid assay kit (Boster Biological Technology). A total of 40 μg of each protein sample was loaded per lane and then separated via 8% SDS-PAGE and transferred onto PVDF membranes (EMD Millipore). After blocking in TBS-0.1% Tween-20 and 5% nonfat dry milk at room temperature for 1 h, the membranes were incubated with rabbit polyclonal anti-ZO-1 antibody (1:1,000; cat. no. 61-3700; Zymed; Thermo Fisher Scientific, Inc.), rabbit anti-HSP70 antibody (1:1,000; cat. no. ab181606; Abcam) and mouse anti-GAPDH antibody (1:2,000; cat. no. ab8245; Abcam) at 4˚C overnight. After rinsing with TBS-0.1% Tween 20, membranes were then incubated HRP-conjugated goat anti-rabbit IgG (1:5,000; cat. no. ab6721; Abcam) and HRP-conjugated goat anti-mouse IgG (1:5,000; cat. no. ab6789; Abcam) at room temperature for 2 h. Finally, the membranes were washed four times and developed using an Immobilon Western Chemiluminescent HRP Substrate kit (EMD Millipore). Gray value analysis was performed using QuantityOne software version 4.6.8 (Bio-Rad Laboratories, Inc.).

H&E staining. Paraffin-embedded sections (5 μm) were prepared as described above. After conventional gradient dewaxing, three sections containing the frontal cortex from each rat (total of 18 sections of each group) were stained in hematoxylin staining solution for 5 min. Following rinsing with tap water for 2 min, sections were placed in an alcohol hydrochloride differentiation fluid for 10 sec and rinsed with tap water for ~10 min until the blue color returned. Then, the sections were stained with eosin for 1 min, then washed with distilled water and dehydrated with gradient alcohol. Finally, the sections were rendered transparent with xylene and sealed with neutral gum. All procedures were performed at room temperature. The morphology of brain tissue was observed in five random visual fields of each section using a light microscope (Nikon Corporation; total magnification, x200).

Statistical analysis. The normality of variables was evaluated using Lilliefors test. Data were expressed as the mean ± SD if they were normally distributed (S100β concentration, relative amount of HSP70 and ZO-1). If non-normally distributed (CS of EB fluorescence, CS of albumin immunohistochemistry), the data were expressed as the median (interquartile range). One-way ANOVA and Tukey's multiple comparison test were applied for comparisons of normally distributed data, whereas Kruskal-Wallis H test followed by Dunn-Bonferroni test for post hoc comparisons was used to analyze non-distributed data. All data were analyzed using SPSS 22.0 software (IBM Corp.), and $P<0.05$ was considered to indicate a statistically significant difference.

Results

Influence of a single UWB-EMP exposure on BBB permeability at different time periods after exposure. The permeability of the BBB was evaluated via EB and albumin extravasation into the brain parenchymal cells, and the levels of S100β in serum at different time periods after a single exposure to UWB-EMP at the field strength of 400 kV/m. The fluorescence images of EB in sham-exposed controls revealed very few or no red fluorescence spots, which are indicative of perivascular albumin leakage, in the cortex (Fig. 1A). In animals exposed to UWB-EMP, there was a greater number of fluorescence spots at 0.5 h, which was further increased at 3 and 6 h. However, at 24 h after UWB-EMP exposure, the leakage was similar to that observed in sham-exposed controls (Fig. 1A). The CS for EB fluorescence in 3 h post-exposure group [6.625 (6.000, 7.313); P=0.001] and 6 h post-exposure group [6.125 (5.375, 6.500); P=0.013] was significantly higher compared with the sham group [0.000 (0.000, 1.625); Fig. 1A]. The CSs obtained from immunohistochemical analysis of albumin extravasation showed perivascular albumin leakage at 0.5 h after UWB-EMP exposure [5.500 (5.000, 6.000); P=0.535] compared with the sham group [0.000 (0.000, 0.125); Fig. 1B]. At 3 h after exposure, both the number of microvessels with albumin exudation and the extent of exudation increased [10.250 (10.188, 10.750); P=0.001], and the CS of albumin extravasation peaked at 6 h [10.500 (10.188, 11.375); P=0.003]. However, at 24 h, albumin distribution in UWB-EMP-exposed animals resembled that in sham-exposed controls (Fig. 1B). The levels of S100β in serum were also

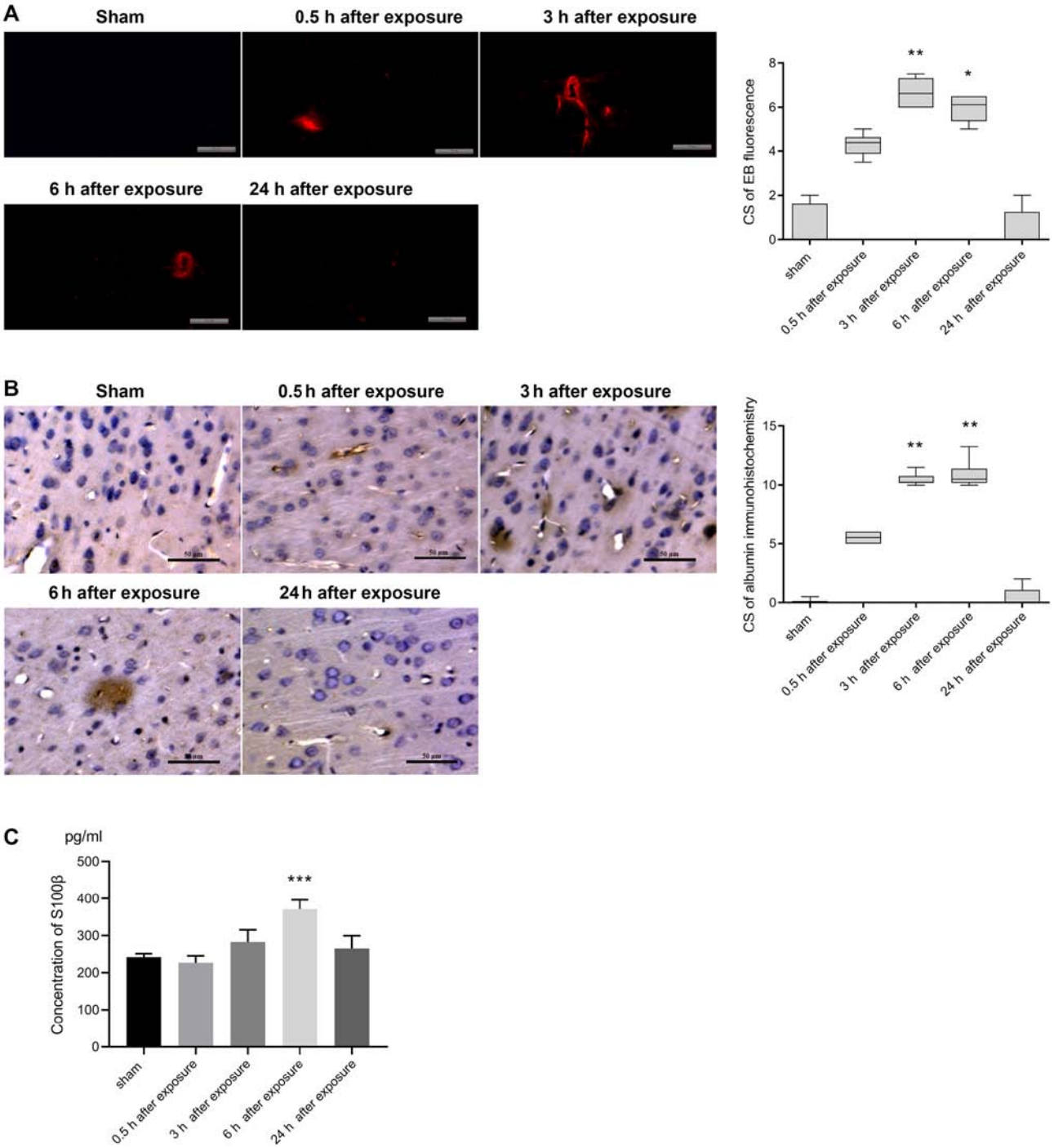

Figure 1. (A) EB fluorescence and (B) albumin immunohistochemical staining of the cerebral cortex of rats at different time points after a single UWB-EMP exposure (scale bar=50 μm) and the CSs for EB staining and albumin immunohistochemistry are presented as the median (interquartile range). (C) Serum S100β levels in rats at different time points after UWB-EMP exposure. The concentration of serum S100β is presented as the mean ± SD. *P<0.05, **P<0.01, ***P<0.001 vs. sham group. CS, comprehensive score; EB, Evans blue; UWB-EMP, ultra-wide band electromagnetic pulse.

significantly increased at 6 h after UWB-EMP exposure (371.292±25.190 ng/ml; P<0.001), while at other exposure time points, there was no significant difference between UWB-EMP-exposed and sham-exposed animals (Fig. 1C).

Influence of UWB-EMP field strength on BBB. Following the observation that the highest increase in BBB permeability occurred between 3 and 6 h after a single UWB-EMP exposure, the influence of field strength on the BBB was then examined. The CSs for albumin immunostaining and EB fluorescence in sham-exposed animals were not significantly difference compared with those exposed to UWB-EMP at 50 kV/m (Fig. 2). However, when UWB-EMP exposure was conducted with a field strength of 200 or 400 kV/m, marked perivascular extravasation of albumin and EB fluorescence was observed in the cerebral cortex of the rats (Fig. 2). The CSs of EB fluorescence and exudation of albumin in animals exposed to UWB-EMP at 400 kV/m [9.250 (8.688, 11.813) and 10.125 (9.875, 12.313), respectively] were notably increased compared with in the 200 kV/m UWB-EMP group [6.375

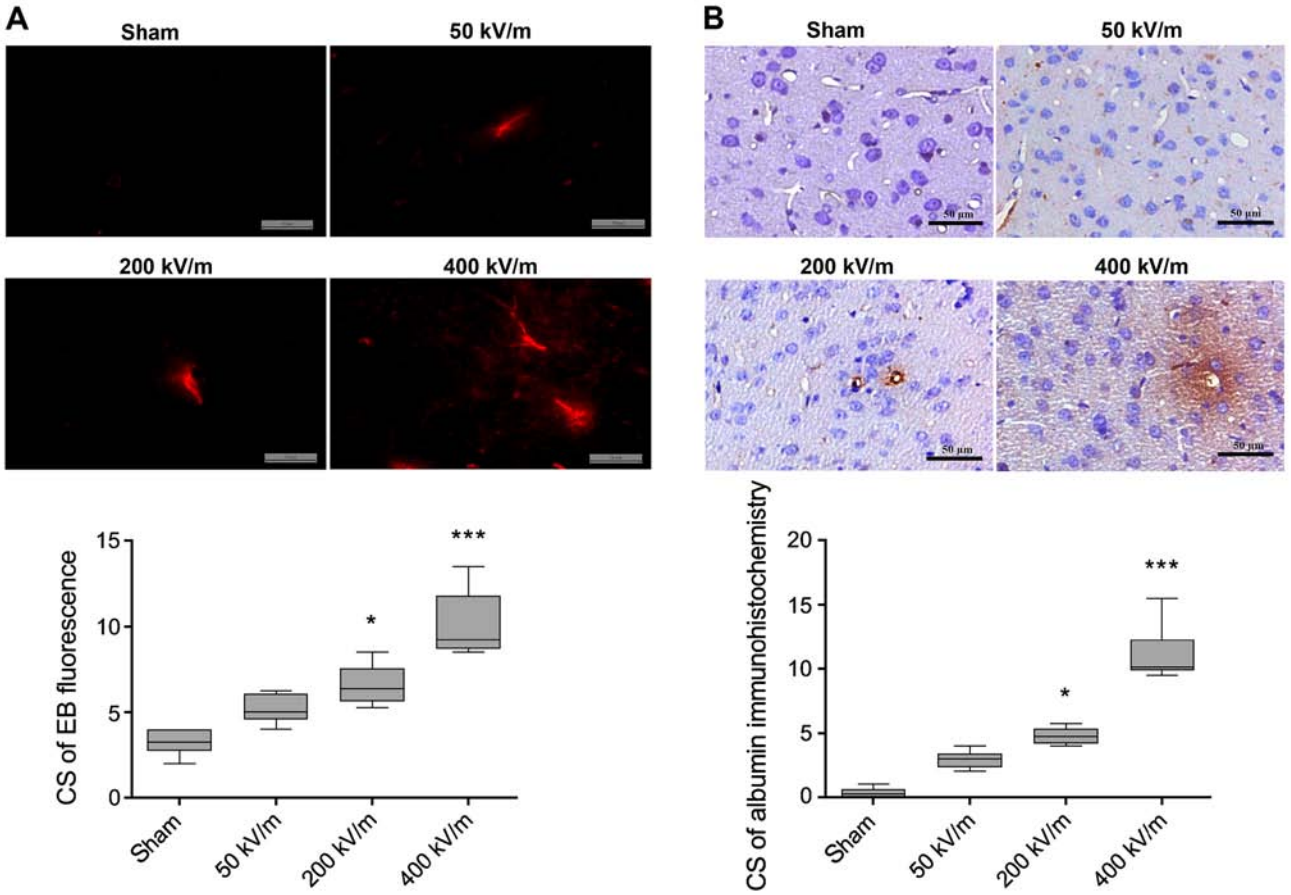

Figure 2. (A) EB fluorescence and (B) albumin immunohistochemical staining of the cerebral cortex of rats after ultra-wide band electromagnetic pulse exposure with different electric field strengths (scale bar=50 μm) and the CSs for EB staining and albumin immunohistochemistry are presented as the median (interquartile range). *P<0.05, ***P<0.001 vs. sham group. CS, comprehensive score; EB, Evans blue.

(5.625, 7.563) and 4.750 (4.188, 5.375), respectively] although the differences were not statistically significant (P=0.637 and P=0.813, respectively; Fig. 2).

Effect of UWB-EMP exposure on ZO-1 in the cortex. ZO-1 is a major TJ protein important for maintaining BBB permeability in the brain (23). Western blot analysis was conducted to evaluate the expression of ZO-1, while immunohistochemical staining was performed to observe the distribution of ZO-1. The results showed that the expression levels of ZO-1 at 3 and 6 h after UWB-EMP exposure (0.942±0.025 and 0.871±0.033, respectively) were significantly decreased (P=0.012 and P<0.001, respectively) and, at 24 h after UWB-EMP exposure, the expression of ZO-1 (0.984±0.025) was slightly lower than that of sham-exposed controls (the difference was not statistically significant; P=0.758; Fig. 3B). However, the distribution of ZO-1 did not notably vary at different exposure time points following UWB-EMP exposure (Fig. 3A).

Effect of UWB-EMP on HSP70 levels in cortex. Western blot analysis of HSP70 expression showed that the expression levels of HSP70 at different time points after UWB-EMP exposure were not significantly altered (Fig. 4A).

Effect of UWB-EMP on the morphology of cerebral cortex. The safety of UWB-EMP exposure was evaluated by analyzing morphological changes in H&E-stained cerebral cortex sections. The data indicated no markedly histopathological abnormalities in any animals exposed to UWB-EMP (Fig. 4B).

Discussion

The development of safe and effective technology to permit access through the BBB is of paramount importance to combating CNS diseases. Oscar and Hawkins (24) observed that a single exposure of rats to 1.3 GHz of continuous or pulsed microwave radiation can increase the permeability of the BBB in the medulla, cerebellum and hypothalamus, but not in the hippocampus and cortex. Albert and Kerns (25) also observed reversible opening of the BBB in random areas of the brains of hamsters exposed to 2.45 GHz microwave radiation. A number of other *in vitro* and *in vivo* studies in rats reported similar observations of enhanced permeability of the BBB (26-29). Conversely, Soderqvist *et al* (30,31) conducted studies in humans, using serum S100β, transthyretin and β-trace protein as markers to examine the impact of 890 MHz microwave radiation on BBB integrity; however, they failed to observe an association or an effect of microwave exposure on the human BBB. These contradictory results may be due to differences in experimental subjects, varying methodologies and, most importantly, diverse microwave exposure parameters. Furthermore, most of the studies that reported impaired

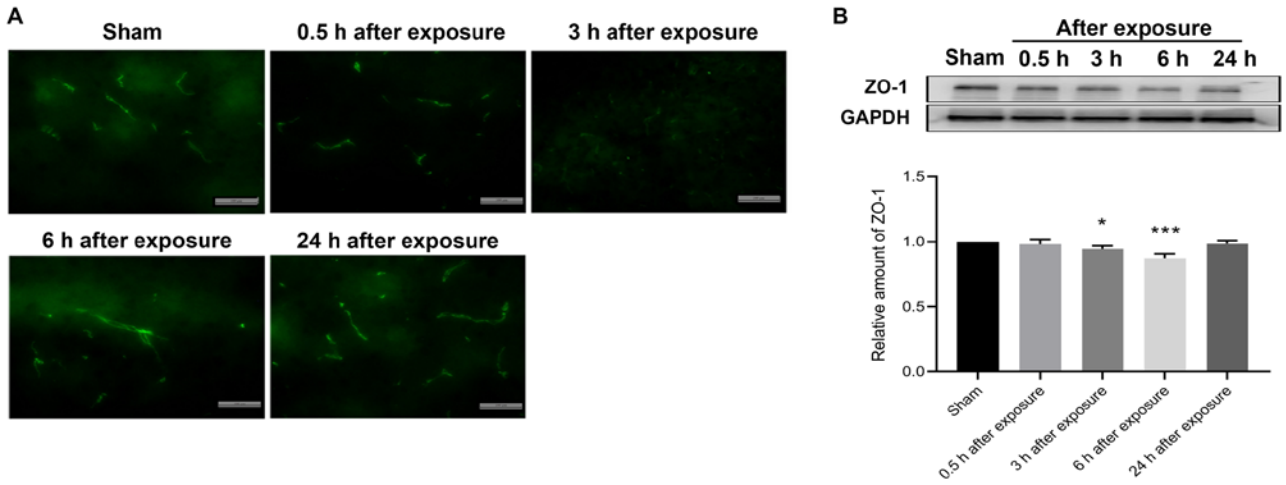

Figure 3. (A) Distribution and (B) expression of ZO-1 in the rat cerebral cortex at different time points after ultra-wide band electromagnetic pulse exposure (scale bar=100 μm, the relative amount of ZO-1 is presented as the mean ± SD). *P<0.05, ***P<0.001 vs. sham group. ZO-1, zonula occludens 1.

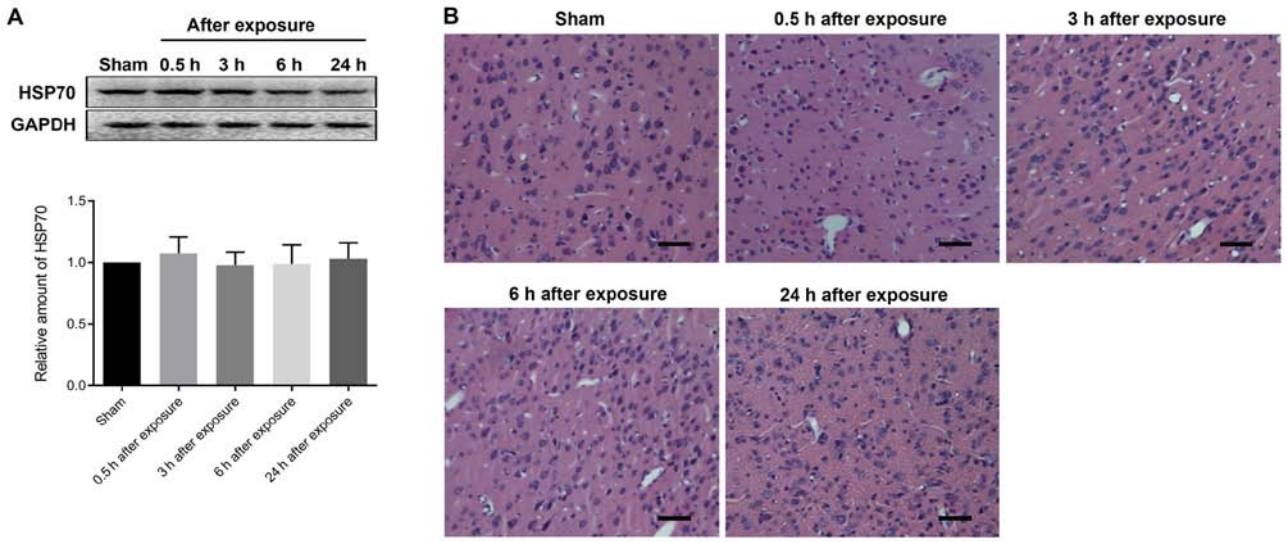

Figure 4. (A) Expression of HSP70 in rat cerebral cortex and (B) H&E staining at different time points after ultra-wide band electromagnetic pulse exposure (magnification, x200; scale bar=50 μm, the relative amount of HSP70 is presented as the mean ± SD). HSP, heat shock protein 70.

BBB integrity following exposure to microwaves focused on adverse effects of long-term exposure and did not consider the thermal effect of microwave radiation, which can damage normal tissue seriously. The ideal microwave exposure that can be applied to assist drugs in penetrating the BBB is preferably a single non-thermal exposure.

UWB-EMP is widely used in radar technology, electronic countermeasures and wireless communications (32). They have a sub-nsec rise time and a pulse width within a small number of nsec. The ultra-short rise time results in its ultra-wide spectrum, and the ultra-short pulse width allows a high peak power density without producing hyperthermia (33). Therefore, the influence of a single UWB-EMP exposure of varying electric field strength was examined on BBB permeability in the present study. The results indicated that the BBB permeability of rats began to increase immediately after UWB-EMP exposure, reaching a maximum between 3-6 h after exposure and returning to normal within 24 h. Subsequent experiments indicated that UWB-EMP exposure with different field strength induced field strength-dependent effects on BBB permeability, as BBB permeability increased with increasing UWB-EMP field strength.

S100β is a protein secreted by glial cells (34). Generally, the concentration of S100β in peripheral blood is very low; a clinical cutoff value ≤0.10 μg/l has been considered normal (35). When the BBB is damaged, S100β can enter the circulatory system in large quantities; thus, the S100β concentration in serum can indirectly reflect the degree of BBB disruption (36). As the biological half-life of plasma S100β is 1-2 h (24), its content also indicates the cumulative degree of BBB opening. In the present study, the S100β concentration in the serum was increased significantly at 6 h after UWB-EMP exposure, which was similar to the results of the albumin immunohistochemistry experiments.

HSP70 is a major stress-inducible protein, which can be induced by stimuli such as injury, heat and ultraviolet exposure (37). The upregulation of HSP70 often indicates a stress state or even disease state (37). In the present study, the expression

levels of HSP70 and brain histomorphology were analyzed to evaluate the safety of a single UWB-EMP exposure. The results indicated that UWB-EMP did not induce significant damage in the brain tissue of rats. Kovacs *et al* (38) reported that BBB opening induced by MRI-guided focused ultrasound combined with microbubbles resulted in an immediate damage-associated molecular pattern response, including elevated HSP70 levels. Compared with focused ultrasound combined with microbubbles, UWB-EMP exposure may cause insufficient damage in the brain to induce expression of HSP70. However, a comprehensive safety evaluation needs to be conducted.

The extensive TJs between BMECs are the structural basis of the BBB, regulating the diffusion of water, ions and macromolecules through the paracellular pathway (39). TJ consists of transmembrane proteins, cytoplasmic accessory proteins and cytoskeletal proteins (39). The ZO proteins are amongst the most integral cytoplasmic accessory proteins, which play a role in connecting transmembrane proteins to cytoskeletal proteins, signal transduction and transcriptional modulation (40). In the present study, the expression and distribution of ZO-1, a 220-kDa protein belonging to the ZO protein family, were evaluated. Previous studies have shown that the abnormal expression or distribution of ZO-1 can lead to TJ integrity disruption, causing an increase in BBB permeability (41-44). In the present study, western blot and immunofluorescence analyses were conducted to determine whether ZO-1 was involved in the disruption of BBB permeability following UWB-EMP exposure. The results indicated that the expression of ZO-1 was decreased significantly at 3 and 6 h after exposure. However, there was no notable effect on its distribution. The parallel changes in ZO-1 expression and BBB integrity suggested an important role for ZO-1 in UWB-EMP-induced BBB opening in the rat brain.

Nevertheless, the present study has certain limitations. Although EB and albumin are common tracers to examine BBB leakage, their large molecular weights (~67 kDa) make it difficult to detect very small increases in BBB permeability. The use of tracers across a varied size range should be considered in further studies. Additionally, the present study only examined a single UWB-EMP exposure. However, further investigations into the impact of repeated and long-term exposure to UWB-EMP are required to find an effective field strength and time period during which BBB permeability is increased.

In conclusion, UWB-EMP exposure increased BBB permeability transiently and safely in a field strength-dependent manner. This was associated with changes in the expression of ZO-1, which could be a mechanism involved in BBB permeability.

Acknowledgements

We wish to acknowledge Dr Hu Long (School of Electronic Science and Engineering, Xi'an Jiaotong University) and Mr Xu Shenglong (Faculty of Preventive Medicine, Airforce Medical University) for their contribution to the maintenance and administration of the UWB-EMP equipment.

Funding

The present study was supported by the National Natural Science Foundation of China (grant no. 51437008).

Availability of data and materials

The datasets used and/or analyzed during the current study are available from the corresponding author on reasonable request.

Authors' contributions

GG and GD conceived the study. PG and QC designed the study, and performed the western blot analysis and ELISA. YL, QG and HY performed H&E staining and immunohistochemical staining. JinL provided UWB-EMP equipment, performed exposure protocols and confirmed the exposure parameters in the study. JH and JiaL performed analysis of data. YZ and LZ helped interpret the staining data and create the figures. GG and GD curated data. PG drafted the original version of the manuscript. LZ, GD and GG revised the manuscript critically. All authors read and approved the final manuscript.

Ethics approval and consent to participate

All experiments were conducted in accordance with the National Institutes of Health Guide for the Care and Use of Laboratory Animals and approved by the Animal Experimentation Ethics Committee of Airforce Medical University (approval no. IACUC-20180503).

Patient consent for publication

Not applicable.

Competing interests

The authors declare that they have no competing interests.

References

1. Hahad O, Lelieveld J, Birklein F, Lieb K, Daiber A and Munzel T: Ambient air pollution increases the risk of cerebrovascular and neuropsychiatric disorders through induction of inflammation and oxidative stress. Int J Mol Sci 21: E4306, 2020.
2. The Lancet Neuroiogy: Global analysis of neurological disease: Burden and benefit. Lancet Neurol 16: 857, 2017.
3. Ostrom QT, Gittleman H, Liao P, Rouse C, Chen Y, Dowling J, Wolinsky Y, Kruchko C and Barnholtz-Sloan J: CBTRUS statistical report: Primary brain and central nervous system tumors diagnosed in the United States in 2007-2011. Neuro Oncol 16 (Suppl 4): iv1-iv63, 2014.
4. Arvanitis CD, Ferraro GB and Jain RK: The blood-brain barrier and blood-tumour barrier in brain tumours and metastases. Nat Rev Cancer 20: 26-41, 2019.
5. Hawkins BT and Davis TP: The blood-brain barrier/neurovascular unit in health and disease. Pharmacol Rev 57: 173-185, 2005.
6. Tang Z, Guo D, Xiong L, Wu B, Xu X, Fu J, Kong L, Liu Z and Xie C: TLR4/PKCα/occludin signaling pathway may be related to blood-brain barrier damage. Mol Med Rep 18: 1051-1057, 2018.
7. Lee MR and Jayant RD: Penetration of the blood-brain barrier by peripheral neuropeptides: New approaches to enhancing transport and endogenous expression. Cell Tissue Res 375: 287-293, 2019.
8. Zhao Z, Nelson AR, Betsholtz C and Zlokovic BV: Establishment and dysfunction of the blood-brain barrier. Cell 163: 1064-1078, 2015.
9. Zhan W and Wang CH: Convection enhanced delivery of chemotherapeutic drugs into brain tumour. J Control Release 271: 74-87, 2018.

10. Parodi A, Rudzinska M, Deviatkin AA, Soond SM, Baldin AV and Zamyatnin AA Jr: Established and emerging strategies for drug delivery across the blood-brain barrier in brain cancer. Pharmaceutics 11: 245, 2019.
11. McDannold N, Zhang Y, Supko JG, Power C, Sun T, Peng C, Vykhodtseva N, Golby AJ and Reardon DA: Acoustic feedback enables safe and reliable carboplatin delivery across the blood-brain barrier with a clinical focused ultrasound system and improves survival in a rat glioma model. Theranostics 9: 6284-6299, 2019.
12. Semyachkina-Glushkovskaya O, Chehonin V, Borisova E, Fedosov I, Namykin A, Abdurashitov A, Shirokov A, Khlebtsov B, Lyubun Y, Navolokin N, *et al*: Photodynamic opening of the blood-brain barrier and pathways of brain clearing. J Biophotonics 11: e201700287, 2018.
13. Ding GR, Qiu LB, Wang XW, Li KC, Zhou YC, Zhou Y, Zhang J, Zhou JX, Li YR and Guo GZ: EMP-induced alterations of tight junction protein expression and disruption of the blood-brain barrier. Toxicol Lett 196: 154-160, 2010.
14. McMahon D, Poon C and Hynynen K: Evaluating the safety profile of focused ultrasound and microbubble-mediated treatments to increase blood-brain barrier permeability. Expert Opin Drug Deliv 16: 129-142, 2019.
15. Kimura S, Kuroiwa T, Ikeda N, Nonoguchi N, Kawabata S, Kajimoto Y and Ishikawa T: Assessment of safety of 5-aminolevulinic acid-mediated photodynamic therapy in rat brain. Photodiagnosis Photodyn Ther 21: 367-374, 2018.
16. Zhou JX, Ding GR, Zhang J, Zhou YC, Zhang YJ and Guo GZ: Detrimental effect of electromagnetic pulse exposure on permeability of in vitro blood-brain-barrier model. Biomed Environ Sci 26: 128-137, 2013.
17. Zhou Y, Qiu LB, An GZ, Zhou JX, Du L, Ma YH, Guo GZ and Ding GR: Effects of electromagnetic pulse exposure on gelatinase of blood-brain barrier in vitro. Electromagn Biol Med 36: 1-7, 2017.
18. Li K, Zhang K, Xu S, Wang X, Zhou Y, Zhou Y, Gao P, Lin J, Ding G and Guo G: EMP-induced BBB-disruption enhances drug delivery to glioma and increases treatment efficacy in rats. Bioelectromagnetics 39: 60-67, 2018.
19. Liang X, Wang Y, Wu S and Gulliver TA: Experimental study of wireless monitoring of human respiratory movements using UWB impulse radar systems. Sensors (Basel) 18: 3065, 2018.
20. National Research Council (US) Committee for the Update of the Guide for the Care and Use of Laboratory Animals: Guide for the care and use of laboratory animals. 8th edition. Washington (DC): National Academies Press (US), 2011.
21. Jiang DP, Li J, Zhang J, Xu SL, Kuang F, Lang HY, Wang YF, An GZ, Li JH and Guo GZ: Electromagnetic pulse exposure induces overexpression of beta amyloid protein in rats. Arch Med Res 44: 178-184, 2013.
22. Wang HL and Lai TW: Optimization of evans blue quantitation in limited rat tissue samples. Sci Rep 4: 6588, 2014.
23. Liu WY, Wang ZB, Zhang LC, Wei X and Li L: Tight junction in blood-brain barrier: An overview of structure, regulation, and regulator substances. CNS Neurosci Ther 18: 609-615, 2012.
24. Oscar KJ and Hawkins TD: Microwave alteration of the blood-brain barrier system of rats. Brain Res 126: 281-293, 1977.
25. Albert EN and Kerns JM: Reversible microwave effects on the blood-brain barrier. Brain Res 230: 153-164, 1981.
26. Zhang YM, Zhou Y, Qiu LB, Ding GR and Pang XF: Altered expression of matrix metalloproteinases and tight junction proteins in rats following PEMF-Induced BBB permeability change. Biomed Environ Sci 25: 197-202, 2012.
27. Tang J, Zhang Y, Yang L, Chen Q, Tan L, Zuo S, Feng H, Chen Z and Zhu G: Exposure to 900 MHz electromagnetic fields activates the mkp-1/ERK pathway and causes blood-brain barrier damage and cognitive impairment in rats. Brain Res 1601: 92-101, 2015.
28. Wang LF, Li X, Gao YB, Wang SM, Zhao L, Dong J, Yao BW, Xu XP, Chang GM, Zhou HM, *et al*: Activation of VEGF/Flk-1-ERK pathway induced blood-brain barrier injury after microwave exposure. Mol Neurobiol 52: 478-491, 2015.
29. Sirav B and Seyhan N: Effects of GSM modulated radio-frequency electromagnetic radiation on permeability of blood-brain barrier in male & female rats. J Chem Neuroanat 75: 123-127, 2016.
30. Soderqvist F, Carlberg M and Hardell L: Use of wireless telephones and serum S100B levels: A descriptive cross-sectional study among healthy Swedish adults aged 18-65 years. Sci Total Environ 407: 798-805, 2009.
31. Soderqvist F, Carlberg M and Hardell L: Biomarkers in volunteers exposed to mobile phone radiation. Toxicol Lett 235: 140-146, 2015.
32. Dorsey WC, Ford BD, Roane L, Haynie DT and Tchounwou PB: Induced mitogenic activity in AML-12 mouse hepatocytes exposed to low-dose ultra-wideband electromagnetic radiation. Int J Environ Res Public Health 2: 24-30, 2005.
33. Ruan C, Zhao W, Chen GF and Zhu SL: Characteristic of the ultra-wideband electromagnetic radiation generated by PCSS. Microwave Opt Technol Lett 49: 1118-1122, 2007.
34. Michetti F, D'Ambrosi N, Toesca A, Puglisi MA, Serrano A, Marchese E, Corvino V and Geloso MC: The S100B story: From biomarker to active factor in neural injury. J Neurochem 148: 168-187, 2019.
35. Astrand R and Unden J: Clinical Use of the Calcium-Binding S100B Protein, a Biomarker for Head Injury. Methods Mol Biol 1929: 679-690, 2019.
36. Kanner AA, Marchi N, Fazio V, Mayberg MR, Koltz MT, Siomin V, Stevens GH, Masaryk T, Aumayr B, Vogelbaum MA, *et al*: Serum S100beta: A noninvasive marker of blood-brain barrier function and brain lesions. Cancer 97: 2806-2813, 2003.
37. Yun CW, Kim HJ, Lim JH and Lee SH: Heat shock proteins: Agents of cancer development and therapeutic targets in anti-cancer therapy. Cells 9: 60, 2019.
38. Kovacs ZI, Kim S, Jikaria N, Qureshi F, Milo B, Lewis BK, Bresler M, Burks SR and Frank JA: Disrupting the blood-brain barrier by focused ultrasound induces sterile inflammation. Proc Natl Acad Sci USA 114: E75-E84, 2017.
39. Haseloff RF, Dithmer S, Winkler L, Wolburg H and Blasig IE: Transmembrane proteins of the tight junctions at the blood-brain barrier: Structural and functional aspects. Semin Cell Dev Biol 38: 16-25, 2015.
40. Tietz S and Engelhardt B: Brain barriers: Crosstalk between complex tight junctions and adherens junctions. J Cell Biol 209: 493-506, 2015.
41. Fan X, Jiang Y, Yu Z, Liu Q, Guo S, Sun X, van Leyen K, Ning M, Gao X, Lo EH and Wang X: Annexin A2 plus low-dose tissue plasminogen activator combination attenuates cerebrovascular dysfunction after focal embolic stroke of rats. Transl Stroke Res 8: 549-559, 2017.
42. Goodall EF, Wang C, Simpson JE, Baker DJ, Drew DR, Heath PR, Saffrey MJ, Romero IA and Wharton SB: Age-associated changes in the blood-brain barrier: Comparative studies in human and mouse. Neuropathol Appl Neurobiol 44: 328-340, 2018.
43. Kim BJ, Hancock BM, Bermudez A, Del Cid N, Reyes E, van Sorge NM, Lauth X, Smurthwaite CA, Hilton BJ, Stotland A, *et al*: Bacterial induction of Snail1 contributes to blood-brain barrier disruption. J Clin Invest 125: 2473-2483, 2015.
44. Zihni C, Mills C, Matter K and Balda MS: Tight junctions: From simple barriers to multifunctional molecular gates. Nat Rev Mol Cell Biol 17: 564-580, 2016.